J Mater Sci (2008) 43:887–891
DOI 10.1007/s10853-007-2189-2

A novel way for preparing high surface area silica monolith with bimodal pore structure

Xiaodong Ma · Hongwen Sun · Peng Yu

Received: 30 June 2007 / Accepted: 24 September 2007 / Published online: 31 October 2007

Abstract The crack-free silica monolith with macropores and mesopores has successfully been achieved in the presence of citric acid as nonsurfactant via sol-gel reactions of tetramethoxysilane (TMOS). Citric acid was removed by calcination to afford monolithic bodies with high specific surface area of 648 m^2/g, pore volume of 0.9 cm^3/g. Poly (ethyl glycol) has been used together with citric acid to control the particle aggregation and internal structure. Macropores in the micrometer range originate from the spinodal phase separation and gelation kinetics. Textural mesopores in the 2–8 nm range are controlled through adding citric acid and postsynthesis treatment in ammonia solution. By employing the glycerol as drying control chemical additives (DCCA), cracks of the materials can be successfully avoided.

Introduction

There is a great deal of interest in the synthesis of porous inorganic materials with control of pore sizes due to their fascinating variety in both pore structure and potential applications [1–6]. Drastic progress in the synthesis of ordered mesoporous silica materials has been obtained, the preparation of materials with a simultaneous control of pore structures and morphology on different scales is still a challenging task. Mesoporous silica sphere [7–10], crystals [11–13], thin films [14–18], rods [19], fibers [20, 21], and monoliths [22–28] have been synthesized, These porous materials with a narrow pore size distribution have been synthesized using supramolecular arrays of surfactants [29, 30] or amphiphilic block copolymers [31] as structure-directing agents. They show wide applications in separation, catalysis, optics, and so on. However, for many applications, materials with hierarchical pore structure are desirable. Nakanishi et al. have prepared a double-pore silica gel monolith with interconnected macropores and textural pores in the inorganic skeletons. This kind of material has been successfully applied in high performance liquid chromatography (HPLC) [32–36] and catalysis supports [37], both of which need macropores for mitigating transport resistance and mesopores for obtaining high surface area. Recently, much work has been focused on the technique to adjust the sizes of macropores and mesopores simultaneously. Smått et al. [38] prepared a silica monolith with multimodal hierarchical porosity through a double-templating synthesis route, in which poly (ethyl glycol) (PEG) was used as phase-separation–inducing agent to produce macropores and coexisted cetyltrimethylammoniumbromides was employed as structure-directing agent to obtain mesopores. Among all kinds of the structure-directing agents, the use of neutral surfactant or nonsurfactant has been demonstrated advantageous in solving the problems of ionic surfactant charge-matching or toxicity of some organic amine.

Wei et al. [39] synthesized mesoporous silica materials with D-glucose as a nonsurfactant pore-forming agent. However, the material obtained is not monolith and no macropores coexisted.

In this article, we report a new method in the synthesis of monolithic silica with macropores and mesopores by using TMOS as precursor. Citric acid was used to control the particle aggregation and internal structure together with

X. Ma (✉) · H. Sun · P. Yu
Tianjin Key Laboratory of Environmental Remediation and Pollution Control, College of Environmental Science and Engineering, Nankai University, Tianjin 300071, China
e-mail: maxd@nankai.edu.cn

PEG. As-synthesized silica monolith exhibited high surface area. The glycerol was employed as drying control chemical additives (DCCA), and cracks of the materials can be successfully avoided.

Experimental

Sample preparation

All chemicals were analytical grade and used as received without further purification. The synthesis procedure was as follows. A total of 2.45 g poly (ethyl glycol) (PEG: molecular = 10,000) was dissolved in 25 mL aqueous acetic acid (pH 5.0), and stirred until a homogeneous solution formed. Subsequently, 11 mL tetramethoxysiliane (TMOS) was added and stirred for 30 min, after which 0.31 g citric acid was added and stirred for another 30 min followed by neutralization with ammonia solution to pH of 5.0. Then the solution was transferred into a plastic vessel and allowed to gel at 40 °C. Gelation took place within 2 h, and then the wet gel was aged for 24 h. The aged wet gel was transferred to an autoclave and immersed in 0.01 M aqueous ammonium hydroxide solution. The autoclave was heated up to 120 °C for 10 h. After hydrothermal treatment, the wet gel was washed with water carefully, followed by immersed in glycerol solution for 6 h. The silica monolith obtained was dried at 70 °C for 12 h. Finally it was calcined from room temperature to 550 °C within a heating rate of 2 °C min^{-1} and held at 550 °C for 4 h.

Characterization

The thermogravimetry and differential scanning calorimetry (TG-DSC) analysis was carried out on silica gel after being dried, using a Setaram Labsys-16. The sample was heated progressively from room temperature to 600 °C with a heating rate of 10 °C min^{-1}. Scanning electron microscope (SEM) experiments were performed with a Hitachi-3000N electron microscope for the observation of the macroporous morphology. Nitrogen sorption experiment was performed by a NOVA1200 gas sorption analyzer. Infrared analysis of the samples was recorded on a Nexus 670 (Thermo Nicolet) FTIR.

Results and discussion

Thermal analysis of silica monolith

Figure 1 shows the TG/DSC profile of the as-synthesized silica gel without being calcined. Three distinct weight loss steps can be seen in the TG curve. The first weight loss below 130 °C may be related to desorption of adsorbed water and volatile substances, which is also reflected by the endothermic effect centered at 62 °C in the DSC profile. The second step between 140 and 240 °C is probably ascribed to the decomposition and oxidation of citric acid and glycerol. The third step between 250 and 550 °C can be attributed to the decomposition and combustion of PEG. The last two steps are accompanied by the intense exothermic effect. Above 550 °C, the weight remains constant and has no endo- or exothermal character. Obviously, PEG and citric acid have been totally removed from silica monolith. Therefore, the top temperature of calcination was fixed as 550 °C.

Characteristics of the synthesized silica monolith

The silica monolith with diameter in the range of 10 mm and length of 40 mm was prepared, examples of which are shown in Fig. 2a. The size and shape of the monolith are determined by the size and shape of the vessel used. The macroporous nature of the monoliths is responsible for their white color. The morphology of silica gel skeletons and macropores is given in Fig. 2b. It can be seen that spherical particles are fused to silica gel skeletons associated with disordered macropores. The resulting macropore and skeleton structures are different from those of silica monolith prepared by Nakanishi and Soga [32], who synthesized a silica monolith with interconnected macropores and textural mesoporosity by using water-soluble polymers, such as PEG to control the phase separation and gelation kinetics. In our case, the added citric acid changed the final gel morphology. It can be deduced that the coexistence of citric acid and PEG affects the process of spinodal phase separation.

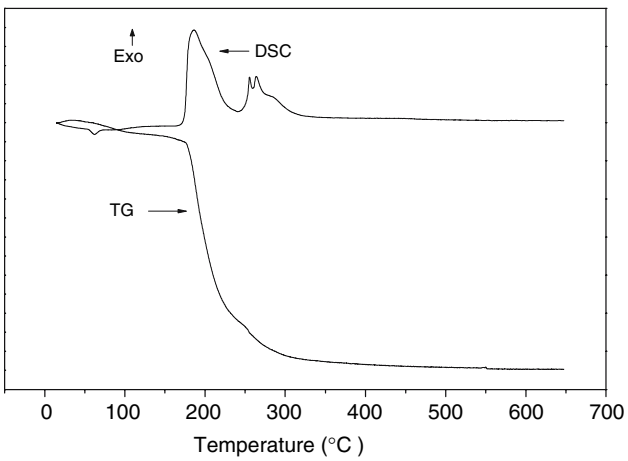

Fig. 1 TG-DSC curves of the silica gel precursor

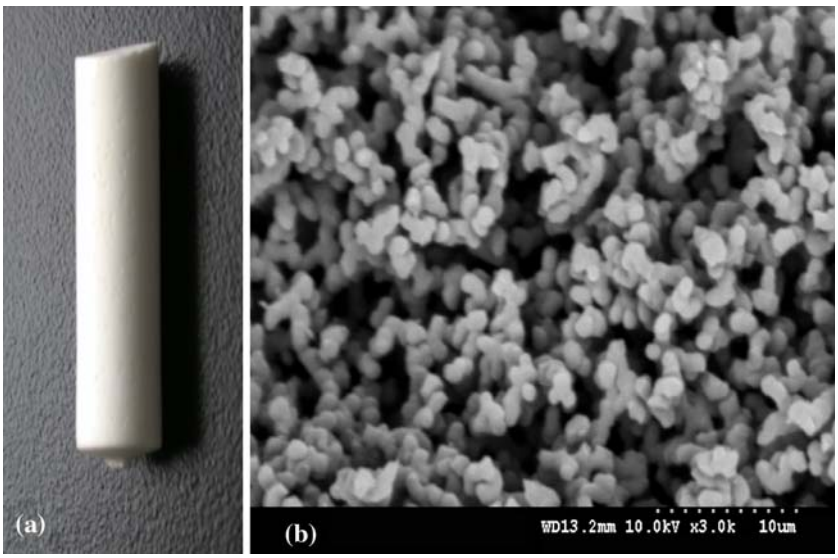

Fig. 2 (**a**) Photograph of the synthesized silica monolith, dimension size: 40 × 10 mm i.d.; (**b**) SEM photograph of typical gel sample

In the process of preparation of silica monolith, the most important problem is obviously the cracking and the shrinkage of the bed during drying. It is difficult to obtain a large size crack-free silica monolith by directly drying a wet silica gel. So drying of the gel is the critical step. The origin of the cracking and shrinkage of the gel have been attributed to capillary pressure generated in micropores in the gel during the drying process. It is believed that gradient in capillary pressure within the pores that leads to mechanical damage; the capillary tension developed during the drying may reach 100–200 Mpa [40] with consequent shrinkage and cracking. The magnitude of the capillary pressure can be expressed by the following equation:

$$\Delta P = 2\gamma\cos\theta/r$$

where γ is the surface tension of the pore liquid at the liquid vapor interface, θ is the contact angle of the liquid, and r is the capillary radius. It is obvious that any changes made to these parameters that tend to minimize the capillary pressure should increase the probability of monolith formation. One alternative is adopting supercritical drying technique with liquid CO_2 to remove the pore liquid from alcogel that is formed by sol-gel process [41]. Supercritical drying has the advantage of sustaining a single fluid phase where drying is free from liquid–vapor interfacial tension, and it facilitates the production crack-free monoliths. The drawback of this method is that the drying must be carried out at high pressure, which needs expensive equipment. Another efficient way of neutralizing the undesired effects of surface stress is to add DCCAs, whose low surface tension tends to reduce capillary pressure.

In this work, wet silica gel was immersed in glycerol solution which was used as DCCA. After immersion for 6 h, the pores are full of glycerol that has a higher viscosity, which facilitates the solvent to vapor at a slow speed at a relatively lower temperature. The network would be uniformly compressed due to the uniform capillary pressure in the gel and no cracking takes place. IR spectra of the gel samples before and after calcination are compared in Fig. 3. According to the previous literatures [42–45], the broad band in the range of 3,800–3,000 cm^{-1} is assigned to a superposition of several stretching modes of Si–OH or H_2O group vibration. The sharp peak at 3,750 cm^{-1} is attributed to isolated, not H-bonded, OH group. The tail band in the 3,650–3,700 cm^{-1} region can be assigned to weakly H-bonded OH groups or internal Si–OH bond. The band in the range of 3,500–3,550 cm^{-1} is linked with silanols forming the hydrogen bonds. The band at 3,200–3,400 cm^{-1} corresponds mainly to adsorbed water. It

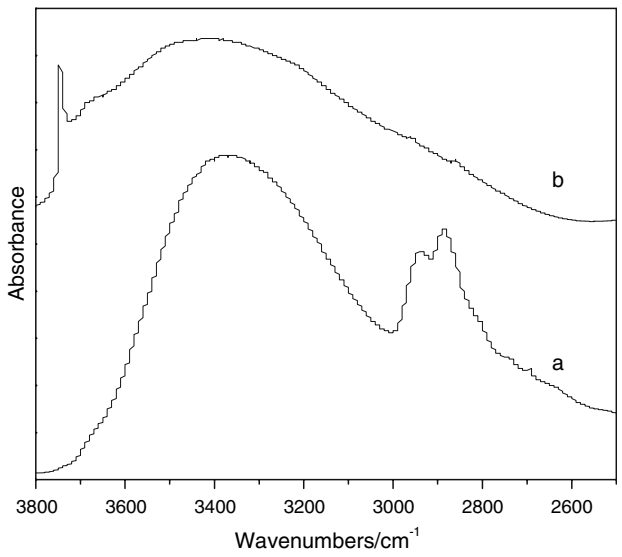

Fig. 3 IR spectra of silica gel before (a) and after (b) calcination

may include strongly disturbed surface hydroxyls forming strong hydrogen bonds Si–O–H–X. The band in the range of 3,000–2,800 cm^{-1} is due to adsorbed substances containing CH groups [46–48]. Compared with the two spectra, it can be seen that, after calcination, the peaks between 2,875 and 2,945 cm^{-1} almost disappeared and the peak at 3,750 cm^{-1} was formed. This indicated that after calcination organic moiety was decomposed completely leading to large amounts of unsaturated Si–O units exposed, forming all kinds of Si–OH and H_2O groups.

Figure 4a shows the nitrogen adsorption/desorption isotherms and the derived pore size distributions of the synthesized silica monolith. The isotherm exhibits a type IV curve with a H_2 type hysteresis loop and a sharp step in the P/P_0 range from 0.6–0.9. This characteristic agrees well with that of mesoporous material reported in the previous literature [49].

The mesopore size distributions were derived from the desorption branch of the N_2 isotherms based on the Barrett–Joyner–Halenda (BJH) method, as shown in Fig. 4b, exhibits a range of 2–8 nm, mean pore diameter of about 5 nm. The specific surface area was 648 m^2/g using Brunauer–Emmett–Teller (BET) method. The total pore volume was 0.87 cm^3/g. It is noticeable that the BET surface area of the silica monolith is much higher than that of silica monolith prepared without adding citric acid.

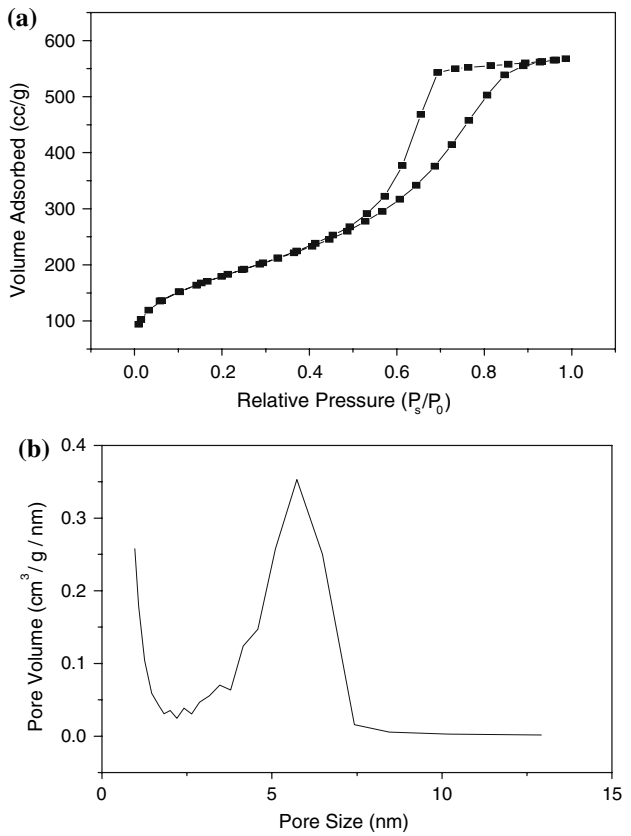

Fig. 4 Nitrogen adsorption/desorption isotherm (**a**) and pore size distribution (**b**) of the silica monolith

Conclusions

A combination of a water-soluble homopolymer and a nonsurfactant has been used to template silica monolith exhibiting macropores in the micrometer range and mesopores in the 2–8 nm range. It is believed that PEG together with citric acid has been used to control the particle aggregation and internal structure. The crack of the monolith can be successfully overcome by immersing the material in glycerol solution which was acted as DCCA. The material with high surface area has a large range of possible applications such as catalysis and separation.

Acknowledgements This study was supported by "100 Projects" of Creative Research for the Undergraduates of Nankai University.

References

1. Corma A (1997) Chem Rev 97:2373
2. Mezza P, Phalippou J, Sempere RJ (1999) J Non-Cryst Solids 243:75
3. Baskaran S, Liu J, Domansky K, Kholer N, Li X, Coyle C, Fryxell GE, Thevuthasan S, Williford RE (2000) Adv Mater 12:291
4. Maschmeyer T (1998) Curr Opin Solid State Mater Sci 3:71
5. Davis ME (1993) Nature 364:391
6. Mosquera MJ, Pore J, Esquivias L, Rivas T, Silva B (2002) J Non-Cryst Solids 311:185
7. Boissiere C, Larbot A, Van der Lee A, Kooyman PJ, Prouzet E (2000) Chem Mater 12:2902
8. Schacht S, Huo Q, Voigt Martin IG, Stucky GD, Schuth F (1996) Science 273:768
9. Huo QS, Feng JL, Schuth F, Stucky GD (1997) Chem Mater 9:14
10. Zhao D, Sun J, Li Q, Stucky GD (2000) Chem Mater 12:275
11. Yu CZ, Tian BZ, Fan J, Stucky GD, Zhao DY (2002) J Am Chem Soc 124:4556
12. Guan S, Inagaki S, Ohsuna T, Terasaki O (2000) J Am Chem Soc 122:5660
13. Che S, Sakamoto Y, Terasaki O, Tatsumi T (2001) Chem Mater 13:2237
14. Yang H, Coombs N, Sokolov I, Ozin GA (1996) Nature 381:589
15. Yang H, Kuperman A, Coombs N, Mamiche Afara S, Ozin GA (1996) Nature 379:703
16. Ogawa M, Ishikawa H, Kikuchi T (1998) J Mater Chem 8:1783
17. Zhao D, Yang P, Melosh N, Feng J, Chmelka BF, Stucky GD (1998) Adv Mater 10:1380
18. Grosso D, Balkenende AR, Albouy PA, Ayral A, Amenitsch H, Babonneau F (2001) Chem Mater 13:1848
19. Yu CZ, Fan J, Tian BZ, Zhao DY, Stucky GD (2002) Adv Mater 14:1742
20. Yang P, Zhao D, Chmelka BF, Stucky GD (1998) Chem Mater 10:2033
21. Marlow F, Spliethoff B, Tesche B (2000) Adv Mater 12:961
22. Feng P, Bu X, Stucky GD, Pine DJ (2000) J Am Chem Soc 122:994
23. Yang H, Shi Q, Tian B, Xie S, Zhang F, Yan Y, Tu B, Zhao D (2003) Chem Mater 15:536

24. Huesing N, Raab C, Torma V, Roig A, Peterlik H (2003) Chem Mater 15:2690
25. Melosh NA, Davidson P, Chmelka BF (2000) J Am Chem Soc 122:823
26. Bagshaw SA, Prouzet E, Pinnavaia TJ (1995) Science 269:1242
27. Templin M, Franck A, Pu Chesne A, Leist H, Zhang Y, Ulrich R, Schadler V, Wiesner U (1997) Science 278:1795
28. Göltner CG, Henke S, Weissenberger MC, Antonietti M (1998) Angew Chem Int Ed 37:613
29. Kresge CT, Leonowicz ME, Roth WJ, Vartuli JC (1992) Nature 359:710
30. Beck JS, Vartuli JC, Roth WJ, Leonowicz ME, Kresge CT, Schmitt KD, Chu CT-W, Olson DH, Sheppard EW, McCullen SB, Higgins JB, Schlenker JL (1992) J Am Chem Soc 114:10834
31. Krämer E, Förster S, Göltner C, Antonietti M (1998) Langmuir 14:2027
32. Nakanishi K, Soga N (1991) J Am Ceram Soc 74:2518
33. Minakuchi H, Nakanishi K, Soga N, Ishizuka N, Tanaka N (1996) Anal Chem 68:3498
34. Minakuchi H, Nakanishi K, Soga N, Ishizuka N, Tanaka N (1997) J Chromatogr A 762:135
35. Minakuchi H, Nakanishi K, Soga N, Ishizuka N, Tanaka N (1998) J Chromatogr A 797:121
36. Minakuchi H, Ishizuka N, Nakanishi K, Soga N, Tanaka N (1998) J Chromatogr A 828:83
37. Chiu JJ, Pine DJ, Bishop ST, Chmelka BF (2004) J Catal 221:400
38. Smått JH, Schunk S, M. Lindén L (2003) Microporous Mesoporous Mater 15:2354
39. Wei Y, Xu J, Dong H, Dong JH, Qiu K, Jansen-Varnum SA (1999) Chem Mater 11:2023
40. Scherer GW, Smith DM (1995) J Non-Cryst Solids 189:197
41. Prassas M, Phalippou J, Zarzycki J (1984) J Mater Sci 19:656
42. Lenza RFS, Vasconcelos WL (2003) J Non-Cryst Solids 330:216
43. Lenza RFS, Vasconcelos WL (2001) Mater Res 4:175
44. Chmel A, Mazurina EK, Shashkin VS (1990) J Non-Cryst Solids 122:285
45. Schraml-Marth M, Walther KL, A.Wokaun (1992) J Non-Cryst Solids 143:93
46. Perry JB (1966) J Phys Chem 70:2937
47. Orcel G, Phalippou J, Hench LL (1986) J Non-Cryst Solids 88:114
48. Parler CM, Ritter JA, Amiridis MD (2001) J Non-Cryst Solids 279:119
49. Sing KSW, Evrett DH, Haul RAW, Moscou L, Pierotti RA, Rouqerol J, Siemieniewska T (1985) Pure Appl Chem 57:603